INFN - Laboratori Nazionali di Frascati, May 1995
From: **The Second DaΦne Physics Handbook**[1]
Chapter 10: Two Photon Processes
Eds. L. Maiani, G. Pancheri, N. Paver

Low-energy photon-photon collisions in chiral perturbation theory

S. Bellucci[1], J. Gasser[2] and M.E. Sainio[3]

[1)] INFN-Laboratori Nazionali di Frascati, P.O.Box 13, I-00044 Frascati, Italy
[2)] Institute for Theoretical Physics, University of Bern, Sidlerstrasse 5, CH-3012 Bern, Switzerland
[3)] Dept. of Theoretical Physics, University of Helsinki, P.O. Box 9 (Siltavuorenpenger 20 C), FIN-00014 Helsinki, Finland

We discuss aspects of the processes

$$\begin{aligned} \gamma\gamma &\rightarrow \pi^+\pi^- \\ \gamma\gamma &\rightarrow \pi^0\pi^0 \end{aligned} \tag{1}$$

in the framework of chiral perturbation theory (CHPT).

1 Introduction

The cross section for $\gamma\gamma \rightarrow \pi\pi$ has been calculated some time ago [1, 2] in the framework of chiral perturbation theory (CHPT) [3] and of dispersion relations. For an early evaluation using effective chiral lagrangians see Ref. [4]. In the case of charged pion-pair production, the chiral calculation [1] at next-to-leading order is in good agreement with the Mark II data [5] in the low-energy region. On the other hand, for $\gamma\gamma \rightarrow \pi^0\pi^0$, the one-loop prediction [1, 2] disagrees with the Crystal Ball data [6] and with dispersion theoretic calculations [7]-[14] even near threshold.

In the process $\gamma\gamma \rightarrow \pi^+\pi^-$, the leading-order contribution[2] is generated by tree diagrams. One has a control on higher order corrections in this case, in the sense that it is

[1]Supported by the INFN, by the EC under the HCM contract number CHRX-CT920026 and by the authors home institutions

[2]We denote the first nonvanishing contribution to any quantity by "the leading-order contribution", independently of whether it starts out at tree level or at higher order in the chiral expansion.

explicitly seen that the one-loop graphs do not modify the tree amplitude very strongly near threshold [1]. Tree diagrams are absent for $\gamma\gamma \to \pi^0\pi^0$ which starts out with one-loop graphs. To establish the region of validity of the chiral representation also in this channel, the amplitude has therefore been evaluated at two-loop order in Ref. [16].

Is a next-to-leading order calculation sufficient in this case? If the corrections are large, the reliability of the result is certainly doubtful. However, a glance at the data shows that the corrections needed to bring CHPT and experiment into agreement are not large – a 25-30% change in amplitude is sufficient. Corrections of this size are rather normal in reactions where pions in an isospin zero S-wave state are present [17]. As an example we mention the isospin zero S-wave $\pi\pi$ scattering length, whose tree-level value [18] receives a 25% correction from one-loop graphs [19]. Corrections of a similar size are present in the scalar form factor of the pion [20].

In the following, we summarize the main results of Refs. [1, 2, 16], considering in particular the cross sections and the pion polarizabilities. For a discussion of $\gamma\gamma \to \pi\pi$ in the framework of generalized chiral perturbation theory, see Ref. [21].

2 Notation

We discuss the processes (1) at lowest order in the electromagnetic interactions, in the isospin symmetry limit $m_u = m_d$. Since the S-matrix element is of order e^2, it follows that $M_{\pi^+} = M_{\pi^0}$ in the approximation considered here. In the following, we use the symbol M_π to denote the charged as well as the neutral pion mass.

The matrix element for *neutral* pion pair production is given by

$$\langle \pi^0(p_1)\pi^0(p_2)\text{out} \mid \gamma(q_1)\gamma(q_2)\text{in}\rangle = i(2\pi)^4\delta^4(P_f - P_i)T^N \quad ,$$

with

$$\begin{aligned} T^N &= e^2\epsilon_1^\mu\epsilon_2^\nu V_{\mu\nu} \quad , \\ V_{\mu\nu} &= i\int dx e^{-i(q_1x+q_2y)}\langle \pi^0(p_1)\pi^0(p_2)\text{out} \mid Tj_\mu(x)j_\nu(y) \mid 0\rangle . \end{aligned}$$

Here j_μ is the electromagnetic current[3]. The decomposition of the correlator $V_{\mu\nu}$ into Lorentz invariant amplitudes reads, with $q_1^2 = q_2^2 = 0$,

$$\begin{aligned} V_{\mu\nu} &= A(s,t,u)T_{1\mu\nu} + B(s,t,u)T_{2\mu\nu} + \cdots \quad , \\ T_{1\mu\nu} &= \frac{s}{2}g_{\mu\nu} - q_{1\nu}q_{2\mu} \quad , \\ T_{2\mu\nu} &= 2s\Delta_\mu\Delta_\nu - \nu^2 g_{\mu\nu} - 2\nu(q_{1\nu}\Delta_\mu - q_{2\mu}\Delta_\nu) \quad , \\ \Delta_\mu &= (p_1 - p_2)_\mu \quad , \end{aligned} \tag{2}$$

[3]We use $e^2/4\pi = \alpha = 1/137.036$. Confusion with the notation for the polarizabilities seems unlikely.

where

$$\begin{aligned}
s &= (q_1+q_2)^2 = 4\boldsymbol{q}^2 = 4(M_\pi^2+\boldsymbol{p}^2) \ , \\
t &= (p_1-q_1)^2 = M_\pi^2 - \frac{s}{2}(1-\sigma(s)\cos\theta) \ , \\
u &= (p_2-q_1)^2 = M_\pi^2 - \frac{s}{2}(1+\sigma(s)\cos\theta) \ , \\
\nu &= t-u \ , \ \sigma(s) = (1-4M_\pi^2/s)^{1/2} \ ,
\end{aligned}$$

are the standard Mandelstam variables, with

$$\boldsymbol{p_1} = -\boldsymbol{p_2} = \boldsymbol{p} \ \ , \ \boldsymbol{q_1} = -\boldsymbol{q_2} = \boldsymbol{q} \ \ , \ \boldsymbol{p}\cdot\boldsymbol{q} = \mid \boldsymbol{p} \mid\mid \boldsymbol{q} \mid \cos\theta \ \ ,$$

in the center-of-mass system. The ellipsis in Eq. (2) denotes terms which do not contribute to the scattering amplitude T^N (gauge invariance). The amplitudes A and B are analytic functions of the variables s, t and u, symmetric under crossing $(t,u) \to (u,t)$. It is useful to introduce in addition the helicity amplitudes

$$\begin{aligned}
H_{++} &= A + 2(4M_\pi^2 - s)B \ , \\
H_{+-} &= \frac{8(M_\pi^4 - tu)}{s}B \ .
\end{aligned}$$

The helicity components H_{++} and H_{+-} correspond to photon helicity differences $\lambda = 0, 2$, respectively. The cross section for unpolarized photons in the center-of-mass system is

$$\begin{aligned}
\sigma^{\gamma\gamma\to\pi^0\pi^0}(s, |\cos\theta| \le Z) &= \frac{\pi\alpha^2}{16}\int_{t_-}^{t_+} dt \ H(s,t) \ , \\
H(s,t) &= \mid H_{++} \mid^2 + \mid H_{+-} \mid^2 \ , \\
t_\pm &= M_\pi^2 - \frac{s}{2}(1 \mp \sigma(s)Z) \ .
\end{aligned}$$

For *charged* pion pair production $\gamma\gamma \to \pi^+\pi^-$, one has

$$\{A, B, H_{+\pm}, H\} \to \{A^C, B^C, H^C_{+\pm}, H^C\}$$

and

$$\sigma^{\gamma\gamma\to\pi^+\pi^-}(s, |\cos\theta| \le Z) = \frac{\pi\alpha^2}{8}\int_{t_-}^{t_+} dt \ H^C(s,t) \ .$$

To set the notation for the polarizabilities, we first consider Compton scattering for charged pions,

$$\gamma(q_1)\pi^\pm(p_1) \to \gamma(q_2)\pi^\pm(p_2) \ , \tag{3}$$

in the laboratory system $p_1^0 = M_\pi$. The electric ($\bar\alpha_\pi$) and magnetic ($\bar\beta_\pi$) polarizabilities are obtained by expanding the Compton amplitude at threshold,

$$T^C = 2\left[\vec\epsilon_1\cdot\vec\epsilon_2^{\,\star}\left(\frac{\alpha}{M_\pi} - \bar\alpha_\pi\omega_1\omega_2\right) - \bar\beta_\pi\,(\vec q_1\times\vec\epsilon_1)\cdot(\vec q_2\times\vec\epsilon_2^{\,\star}) + \cdots\right] \tag{4}$$

with $q_i^\mu = (\omega_i, \vec{q}_i)$. In terms of the helicity components, one has

$$\bar{\alpha}_\pi \pm \bar{\beta}_\pi = -\frac{\alpha}{M_\pi} \bar{H}^C_{+\mp}(s=0, t=M_\pi^2) \ , \tag{5}$$

where the bar denotes the amplitude with the Born term removed[4]. For neutral pions, one uses the analogous definition,

$$\bar{\alpha}_{\pi^0} \pm \bar{\beta}_{\pi^0} = \frac{\alpha}{M_\pi} H_{+\mp}(0, M_\pi^2) \ , \tag{6}$$

or, in terms of A and B,

$$\begin{aligned} \bar{\alpha}_{\pi^0} &= \frac{\alpha}{2M_\pi}(A + 16M_\pi^2 B)|_{s=0,t=M_\pi^2} \ , \\ \bar{\beta}_{\pi^0} &= -\frac{\alpha}{2M_\pi} A|_{s=0,t=M_\pi^2}. \end{aligned} \tag{7}$$

Below we also use the notation

$$\begin{aligned} (\alpha \pm \beta)^C &= \bar{\alpha}_\pi \pm \bar{\beta}_\pi \ , \\ (\alpha \pm \beta)^N &= \bar{\alpha}_{\pi^0} \pm \bar{\beta}_{\pi^0} \ . \end{aligned} \tag{8}$$

An unsubtracted forward dispersion relation for the amplitude B gives

$$(\alpha + \beta)^N = \frac{M_\pi}{\pi^2} \int_{4M_\pi^2}^\infty \frac{ds'}{(s' - M_\pi^2)^2} \sigma_{\text{tot}}^{\gamma\pi^0}(s') \ , \tag{9}$$

and analogously for the charged channel.

3 Low-energy expansion

The evaluation of the amplitude for $\gamma\gamma \to \pi\pi$ in the framework of CHPT is standard [3]. The main points are the following:

1. The underlying effective lagrangian for $SU(2) \times SU(2) \times U(1)$ considered here has the structure [22, 16]
$$\mathcal{L} = \mathcal{L}_2 + \mathcal{L}_4 + \mathcal{L}_6 + \cdots \ ,$$
where the indices denote the number of derivatives, or quark mass terms. The leading term $\mathcal{L}_2$ is the nonlinear sigma-model lagrangian. $\mathcal{L}_4$ contains all possible contributions with four derivatives, or two derivatives and one quark mass term, or two quark mass insertions. These are multiplied with low-energy constants l_i whose divergences absorb the ultraviolet singularities of the one-loop graphs with $\mathcal{L}_2$ [22]. Finally, $\mathcal{L}_6$ contains terms with six derivatives, four derivatives and one quark mass term, etc. [23]. These absorb the ultraviolet divergences of two-loop graphs.

[4] We use the Condon-Shortley phase convention.

2. In the *charged* channel, the leading term is generated by tree diagrams,

$$H_{+\pm}^{C} = H_{+\pm}^{C,\mathrm{tree}} + H_{+\pm}^{C,\mathrm{1loop}} + \cdots \quad , \tag{10}$$

with

$$\begin{pmatrix} H_{++} \\ H_{+-} \end{pmatrix}^{\mathrm{C,tree}} = -4(M_\pi^2 - t)^{-1}(M_\pi^2 - u)^{-1} \begin{pmatrix} M_\pi^2 \\ (M_\pi^4 - tu)/s \end{pmatrix} . \tag{11}$$

The one-loop contribution is [1]

$$\begin{pmatrix} H_{++} \\ H_{+-} \end{pmatrix}^{\mathrm{C,1loop}} = \begin{pmatrix} -2[\bar{G}(s) + 2(2l_5^r - l_6^r)]/F_\pi^2 \\ 0 \end{pmatrix} . \tag{12}$$

where $F_\pi \simeq 93$ MeV is the pion decay constant. The low-energy parameters $2l_5^r, l_6^r$ are from $\mathcal{L}_4$. The combination $2l_5^r - l_6^r$ is scale independent [22]. In the following, we use

$$2l_5^r - l_6^r = 2.85 \cdot 10^{-3} . \tag{13}$$

The same combination of low-energy constants occurs in radiative pion decays at this order in the low-energy expansion [24]. Furthermore, the function $\bar{G}$ is given by

$$-16\pi^2 \bar{G}(s) = \begin{cases} 1 \quad + \frac{M_\pi^2}{s}\left(\ln\frac{1-\sigma}{1+\sigma} + i\pi\right)^2 & ; \quad 4M_\pi^2 \leq s \\ 1 \quad - \frac{4M_\pi^2}{s}\mathrm{arctg}^2(\frac{s}{4M_\pi^2 - s})^{\frac{1}{2}} & ; \quad 0 \leq s \leq 4M_\pi^2 \\ 1 \quad + \frac{M_\pi^2}{s}\ln^2\frac{\sigma-1}{\sigma+1} & ; \quad s \leq 0. \end{cases}$$

3. The leading term in the *neutral* channel is generated by one-loop graphs with $\mathcal{L}_2$,

$$H_{+\pm} = H_{+\pm}^{\mathrm{1loop}} + H_{+\pm}^{\mathrm{2loops}} + \cdots \quad ,$$

with [1, 2]

$$\begin{pmatrix} H_{++} \\ H_{+-} \end{pmatrix}^{\mathrm{1loop}} = \begin{pmatrix} 4(s - M_\pi^2)\bar{G}(s)/sF_\pi^2 \\ 0 \end{pmatrix} . \tag{14}$$

4. The *next-to-leading order* terms in the neutral channel are generated by two-loop, one-loop and tree-diagrams generated by $\mathcal{L}_2, \mathcal{L}_4$ and $\mathcal{L}_6$, respectively. For an evaluation of these and for an explicit expression of the amplitudes see Ref. [16]. The amplitudes contain, at this order in the low-energy expansion, the renormalized constants $l_1^r, \ldots, l_6^r$ and, in addition, three more renormalized parameters $h_\pm^r, h_s^r$ from $\mathcal{L}_6$.

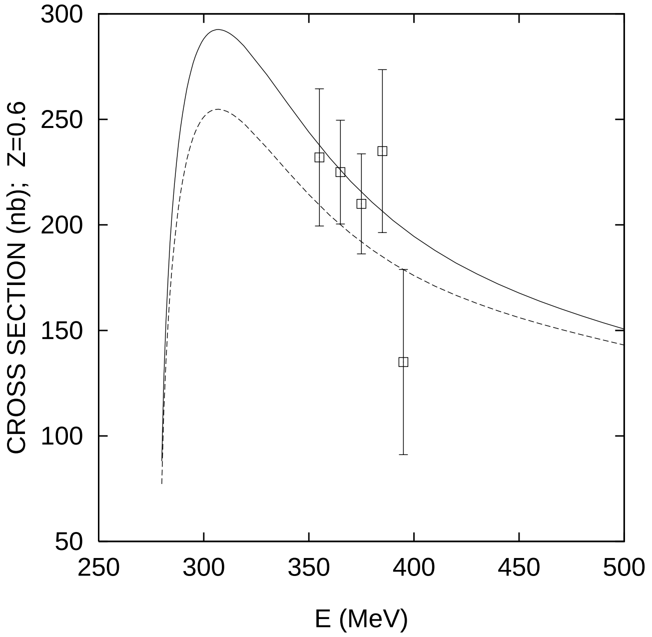

Figure 1: The $\gamma\gamma \to \pi^+\pi^-$ cross section $\sigma(|\cos\theta| \le Z)$ as a function of the center-of-mass energy E at $Z = 0.6$, together with the data from the Mark II collaboration [5]. We have added in quadrature the tabulated statistical and systematic errors. In addition, there is an overall normalization uncertainty of 7% in the data [5]. The dashed line is the Born approximation (10), and the solid line includes the one-loop contribution (12) [1].

5. The constants l_i^r from $\mathcal{L}_4$ are known [22]. On the other hand, those from $\mathcal{L}_6$ have not yet been determined in a systematic manner. The ones which contribute to $\gamma\gamma \to \pi^0\pi^0$, namely $h_\pm^r$ and h_s^r, have been estimated in [16] in the standard manner [3] using resonance exchange with $J^{PC} = 1^{--}, 1^{+-}, 0^{++}, 2^{++}$. For an estimate of a particular contribution to h_+^r by use of sum rules see Ref. [21, 25]. It would be interesting to pin down all three couplings $h_\pm^r$ and h_s^r with this technique. Recently the constants $h_\pm^r$ and h_s^r have been calculated within the Extended Nambu Jona-Lasinio model [26]. The results agree within the uncertainties with the estimate of Ref. [16].

4 The cross section $\gamma\gamma \to \pi^+\pi^-$

Fig. 1 displays the data for the $\gamma\gamma \to \pi^+\pi^-$cross section $\sigma(s; |\cos\theta| \le Z = 0.6)$ as determined by the Mark II collaboration [5]. They are shown as a function of the center-of-mass energy $E = \sqrt{s}$. The dashed line displays the tree-level approximation[5], whereas

[5]In order to take into account physical phase space, we use from here on

$$M_\pi = \begin{cases} 139.57 \ \text{MeV} & \gamma\gamma \to \pi^+\pi^- \ , \quad \gamma\pi^\pm \to \gamma\pi^\pm \\ 134.97 \ \text{MeV} & \gamma\gamma \to \pi^0\pi^0 \ , \quad \gamma\pi^0 \to \gamma\pi^0 \end{cases}$$

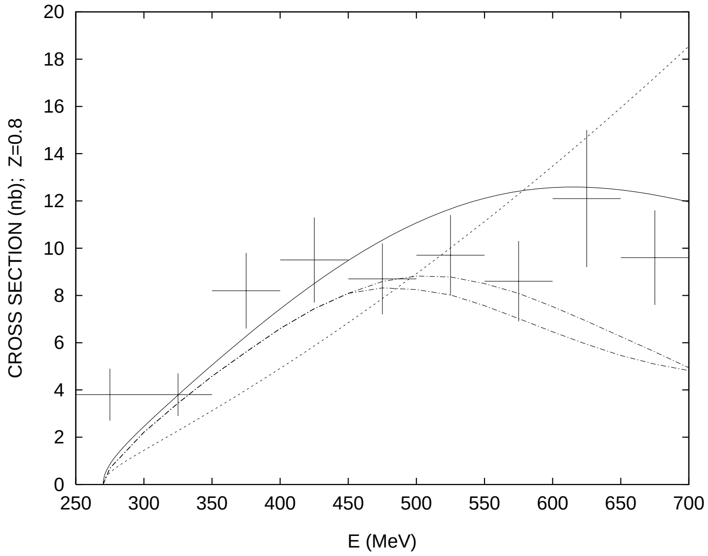

Figure 2: The $\gamma\gamma \to \pi^0\pi^0$ cross section $\sigma(|\cos\theta| \leq Z)$ as a function of the center-of-mass energy E at $Z = 0.8$, together with the data from the Crystal Ball experiment [6]. The solid line is the full two-loop result, and the dashed line results from the one-loop calculation [1, 2]. The band denoted by the dash-dotted lines is the result of the dispersive calculation by Pennington (Fig. 23 in [9]).

the solid line denotes the one-loop result [1] according to Eq. (12). It is seen that the one-loop graphs modify the tree result in the right direction with the correct size. At the same time, the correction is small, of the order of 7% in modulus of the amplitude at $\sqrt{s} = 300$ MeV. This indicates that higher orders will be negligible in this case. All in all, good agreement is achieved with the data in the low-energy region. The low-energy constant $2l_5^r - l_6^6$ has also been determined [27] from the data below 500 MeV, with the result $2l_5^r - l_6^r = (2.4 \pm 1.8) \cdot 10^{-3}$, which is in agreement with the value given in Eq. (13) taken from radiative pion decays. We conclude that the data and the chiral representation in the charged channel agree with each other in the low-energy region.

5 The cross section $\gamma\gamma \to \pi^0\pi^0$

Fig. 2 displays the data for the cross section $\sigma(s; |\cos\theta| \leq Z = 0.8)$ as determined in the Crystal Ball experiment [6]. They are shown as a function of the center-of-mass energy $E = \sqrt{s}$. The dashed line displays the one-loop result [1, 2], evaluated with the amplitudes (14), whereas the solid line denotes the two-loop result [16]. Finally, the dash-dotted lines show the result of a dispersive analysis (Fig. 23 in Ref. [9]). In that calculation, use was made of the $I = 0, 2$ S-wave $\pi\pi$ phase shifts from Ref. [28] (these phase shifts satisfy

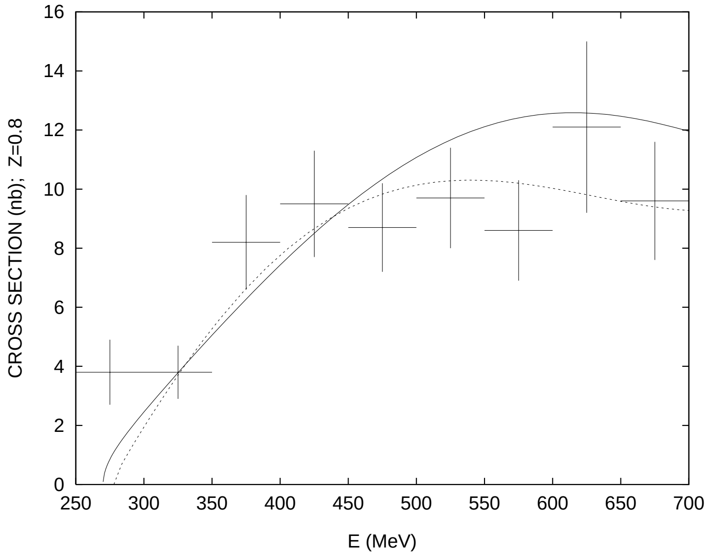

Figure 3: The $\gamma\gamma \rightarrow \pi^0\pi^0$ cross section $\sigma(|\cos\theta| \leq Z)$ as a function of the center-of-mass energy at $Z = 0.8$, with the data from the Crystal Ball [6] experiment. The solid line is the two-loop result, whereas the dashed line is taken from the dispersive analysis of Donoghue and Holstein (Fig. 2 in [10]).

[29] constraints imposed by Roy-type equations). The one-loop result is below the data also near the threshold. This fact created some dust in the literature and in talks given at conferences, to the extent that the validity of CHPT in this process was questioned. However, it is seen that the contributions from the two-loop graphs generate the corrections which are needed to bring the calculation into agreement with the present data and with the dispersive calculation. In this connection, we recall that the low-energy constants $h_{\pm}^r$ and h_s^r contribute very little to the cross section below $E = 450$ MeV [30]-[33]. Their exact value is, therefore, of no concern for the low-energy region in $\gamma\gamma \rightarrow \pi^0\pi^0$. In Fig. 3 is shown a comparison of the two-loop result with the calculation of Donoghue and Holstein [10]. These authors use a dispersive representation of the S-wave projected helicity amplitude and fix the subtraction constant from the chiral representation at order E^4. Contributions from resonance exchange which generate the left-hand cut are also added. The final result for the cross section agrees very well with the two-loop calculation below $E = 400$ MeV. The main differences in the two representations are as follows. First, in the dispersive method, higher order terms are partially summed up. We consider the fact, that the cross sections agree, as an additional indication that yet higher orders in the chiral expansion indeed do not affect very much the amplitude in the threshold region. (In Ref. [16], the uncertainty due to higher orders is estimated at $15\% - 20\%$ in the cross section below 400 MeV.) Secondly, CHPT reveals that the amplitude contains chiral logarithms, generated by pion loops. All of these effects are not incorporated in the dispersive analysis of Refs. [8, 9, 10]–we refer the reader to Ref. [16] for a more detailed discussion of this point.

6 Pion polarizabilities

6.1 Data on pion polarizabilities

The data available are collected and commented in the contribution by Portolés and Pennington [35]. See also Ref. [36].

6.2 Chiral expansion of $\bar{\alpha}_\pi$ and $\bar{\beta}_\pi$

The structure of the quark mass expansion of the polarizabilities is very similar to the one of the threshold parameters in $\pi\pi$ scattering. To illustrate, we consider, in addition to the polarizabilities, also the chiral expansion of the $I = 0$, S-wave scattering length a_0 [18, 19],

$$\begin{array}{rcccccccc}
a_0 & = & \dfrac{7M_\pi^2}{32\pi F_\pi^2}\Bigg\{ & A & + & \dfrac{M_\pi^2 B}{16\pi^2 F_\pi^2} & + & O(M_\pi^4) & + \; O(M_\pi^6)\Bigg\} \;, \\
(\alpha \pm \beta)^{N,C} & = & \dfrac{\alpha}{16\pi^2 F_\pi^2 M_\pi}\Bigg\{ & 0 & + & A_\pm^{N,C} & + & \dfrac{M_\pi^2 B_\pm^{N,C}}{16\pi^2 F_\pi^2} & + \; O(M_\pi^4)\Bigg\} \;. \\
 & & & tree & & 1loop & & 2loops & 3loops
\end{array}$$

The last line indicates the number of loops required to generate the corresponding term in the quark mass expansion. The similarity of the two expansions is obvious – the only difference being that the expansion for the scattering length starts out with tree graphs [18], whereas the leading order term in the polarizabilities are generated by one-loop diagrams [1, 2, 37],

$$A = 1 \;\;,\;\; A_\pm^N = \left(\begin{array}{c} 0 \\ -\frac{1}{3} \end{array}\right) \;\;,\;\; A_\pm^C = \left(\begin{array}{c} 0 \\ 64\pi^2(2l_5^r - l_6^r) \end{array}\right) \;.$$

The next-to-leading order terms B and $B_\pm^N$ have been determined in Ref. [19] and [16], respectively. $B_\pm^N$ contain the low-energy constants $h_\mp^r$ from the order E^6 lagrangian. Work to evaluate the corresponding coefficients $B_\pm^C$ in the charged channel case is in progress [38].

The numerical value for the *leading-order terms* in the expansion of the polarizabilities is[6]

$$\begin{aligned}
(\alpha + \beta)^{N,C} &= 0.0 \;, \\
(\alpha - \beta)^N &= -1.0 \;, \\
(\alpha - \beta)^C &= 5.3 \;.
\end{aligned}$$

The *two-loop* result for the neutral pion case is shown in table 1. The second column contains again the leading order contribution $O(E^{-1})$, whereas the third and fourth ones display the terms of order E. The total values are given in column 5. Finally, the estimates

[6] We express the polarizabilities in units of 10^{-4} fm^3 throughout.

Table 1: Neutral pion polarizabilities to two loops in units of $10^{-4}\mathrm{fm}^3$.

	$O(E^{-1})$	$O(E)$			
	1 loop	$h_{\pm}^r$	2 loops	total	uncertainty
$(\alpha+\beta)^N$	0.00	1.00	0.17	$\simeq 1.15$	± 0.30
$(\alpha-\beta)^N$	-1.01	-0.58	-0.31	$\simeq -1.90$	± 0.20
$\bar{\alpha}_{\pi^0}$	-0.50	0.21	-0.07	$\simeq -0.35$	± 0.10
$\bar{\beta}_{\pi^0}$	0.50	0.79	0.24	$\simeq 1.50$	± 0.20

of the uncertainties are shown in the last column. These correspond to the uncertainty with which the low-energy constants were obtained in Ref. [16], and contain neither effects from higher orders in the quark mass expansion nor any correlations.

For an estimate of pion polarizabilities using dispersion sum rules see [39, 40]. See also [41] for a calculation of the contributions from resonance exchange within CHPT.

Turning now to a comparison with the data, the two-loop results for $(\alpha \pm \beta)^N$ agree within the errors with the values found in [13, 14],

$$\begin{aligned} (\alpha-\beta)^N &= -1.1 \;\pm 1.7 \quad [13] \;, \\ (\alpha+\beta)^N &= \;\; 1.00 \pm 0.05 \quad [14] \quad . \end{aligned} \tag{15}$$

– see, however, the objections made in [35] on the results found in Refs. [13, 14]. As for the charged channel case, we note that the two-loop contribution B_+^N contains (squares of) chiral logarithms [16],

$$B_+^N = \frac{2}{9}\left(\ln\frac{M_\pi^2}{\mu^2} - 96\pi^2 l_2^r\right)\ln\frac{M_\pi^2}{\mu^2} + \cdots \quad ,$$

where μ denotes the scale of renormalization. These are the analogue of the chiral logarithm in the expansion of a_0 [19],

$$B = -\frac{9}{2}\ln\frac{M_\pi^2}{\mu^2} + \cdots \;.$$

The contribution of the chiral logarithms are potentially large. There is no reason why such logarithms should not be present in $B_\pm^C$ as well. Therefore, in order to compare the prediction with the data in a meaningful manner, a full two-loop calculation is required also for the charged channel [38].

6.3 On the determination of polarizabilities from data on $\gamma\gamma \to \pi\pi$

A direct measurement of the Compton amplitude $\gamma\pi \to \gamma\pi$ is difficult to achieve, as is illustrated by the scarce data available on this process. Direct experimental information on the pion polarizabilities is therefore difficult to obtain as well. For this reason, one may seek to determine them instead from data on the crossed channel reaction $\gamma\gamma \to \pi\pi$. Let us compare the mathematical situation with pion-nucleon scattering. Here, the value Σ of the amplitude at the Cheng-Dashen point is of considerable theoretical interest, because it is closely related to the sigma term. It has been shown by the Karlsruhe group [42] that Σ can, also in practice, be obtained from the data on $\pi N \to \pi N$ by analytic continuation. In this language, the determination of the polarizabilities from $\gamma\gamma \to \pi\pi$ amounts to the opposite problem: determine from data on $\pi\pi \to N\bar{N}$ the scattering lengths in $\pi N \to \pi N$. It would be interesting to proceed in a manner similar to the case of pion-nucleon scattering in order to find out whether data on $\gamma\gamma \to \pi\pi$ does or does not suffice to pin down in practice the polarizabilities.

Quite apart from this general setting, one may gain information on the polarizabilities by use of an explicit expression for the amplitude, which serves to interpolate between the Compton threshold and the physical region for $\gamma\gamma \to \pi\pi$. The free parameters in the amplitude are adjusted such that a satisfactory description for $\gamma\gamma \to \pi\pi$ is achieved, which allows one finally to read off the values of the polarizabilities. Examples of this procedure may be found in Refs. [35, 9, 10, 13, 14, 27], for a critical discussion of the method see in particular Ref. [35]. In the case where the chiral representation [16] is used for the interpolation in the neutral channel, the situation is as follows [10]. As we mentioned above, there are three low-energy constants $h^r_\pm, h^r_s$ which enter the amplitude at order E^6. The two parameters $h^r_\pm$ may be traded for the polarizabilities $(\alpha \mp \beta)^N$, whereas h^r_s may be determined e.g. from resonance exchange. It turns out that the cross section in the low-energy region is not very sensitive to the values of the polarizabilities. To illustrate, Fig. 4 displays the cross section at two-loop order for a fixed value $(\alpha+\beta)^N = 1.15$ and a fixed value of h^r_s, varying $(\alpha-\beta)^N$ between -0.95 and -3.8. See also Fig. 10 in Ref. [10]. The sensitivity of the cross section to $(\alpha+\beta)^N$ is even weaker. The charged channel is discussed in Ref. [10], see in particular Fig. 9 in this reference.

We conclude that, in case the chiral amplitude is used as an interpolation in the neutral channel, low-energy data on the cross section alone will not suffice to pin down the neutral pion polarizabilities at this order in the low-energy expansion [35, 10, 16, 21]. On the other hand, the chiral amplitude contains 3 parameters which may be determined by other means [16, 21, 25], see also [26]. Once this is achieved, the process $\gamma\gamma \to \pi^0\pi^0$ serves as a consistency check of the calculation. Using presently available data, we have seen above that the chiral amplitude has successfully passed this check [16].

7 Improvements at DAΦNE

The DAΦNE facility will have the opportunity to test the chiral predictions at next-to-leading order in much more detail than is possible with present data, both in the charged and in the neutral channel.

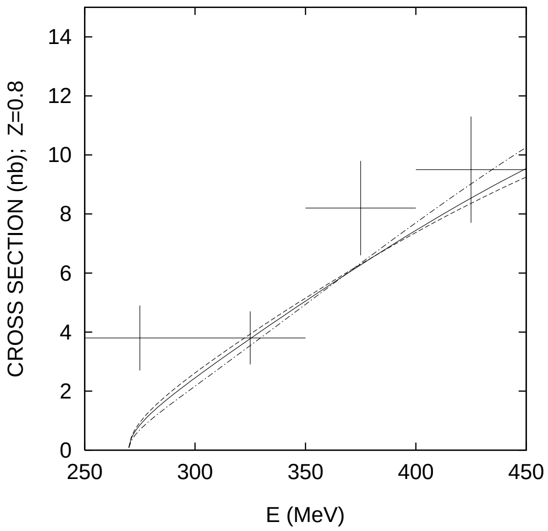

Figure 4: The two-loop result for the cross section $\sigma^{\gamma\gamma\to\pi^0\pi^0}$ at $Z = 0.8$, evaluated with $(\alpha+\beta)^N = 1.15$ and $h_s^r = 7$, varying $(\alpha-\beta)^N$ between $(\alpha-\beta)^N = -0.95$ (dashed line) and $(\alpha-\beta)^N = -3.8$ (dash-dotted line). The solid line corresponds to $(\alpha-\beta)^N = -1.9$ [16]. For additional explaining text see Fig. 3.

References

[1] J. Bijnens and F. Cornet, Nucl. Phys. B296 (1988) 557.

[2] J.F. Donoghue, B.R. Holstein and Y.C. Lin, Phys. Rev. D37 (1988) 2423.

[3] J. Bijnens, G. Ecker and J. Gasser, Chiral perturbation theory, this handbook.

[4] M.K. Volkov and V.N. Pervushin, Yad. Fiz. 22 (1975) 346 (Sov. J. Nucl. Phys. 22 (1975) 179), in particular appendix 1.

[5] The Mark II Collaboration (J. Boyer et al.), Phys. Rev. D42 (1990) 1350.

[6] The Crystal Ball Collaboration (H. Marsiske et al.), Phys. Rev. D41 (1990) 3324.

[7] R.L. Goble, R. Rosenfeld and J.L. Rosner, Phys. Rev. D39 (1989) 3264. The literature on earlier work may be traced from this reference.

[8] D. Morgan and M.R. Pennington, Phys. Lett. B272 (1991) 134.

[9] M.R. Pennington, in [15], p. 379.

[10] J.F. Donoghue and B.R. Holstein, Phys. Rev. D48 (1993) 137.

[11] A. Dobado and J.R. Peláez, Z. Phys. C57 (1993) 501.

[12] T.N. Truong, Phys. Lett. B313 (1993) 221.

[13] A.E. Kaloshin and V.V. Serebryakov, preprint ISU-IAP.Th93-03 (hep-ph/9306224).

[14] A.E. Kaloshin, V.M. Persikov and V.V. Serebryakov, preprint ISU-IAP.Th94-01 (hep-ph/9402220).

[15] The DAΦNE Physics Handbook, Eds. L. Maiani, G. Pancheri and N. Paver (INFN, Frascati, 1992).

[16] S. Bellucci, J. Gasser and M.E. Sainio, Nucl. Phys. B423 (1994) 80.

[17] T.N. Truong, Phys. Rev. Lett. 61 (1988) 2526.

[18] S. Weinberg, Phys. Rev. Lett. 17 (1966) 616; 18 (1967) 188.

[19] J. Gasser and H. Leutwyler, Phys. Lett. B125 (1983) 325.

[20] J. Gasser and U.G. Meißner, Nucl. Phys. B357 (1991) 90.

[21] M. Knecht, B. Moussallam and J. Stern, preprint IPNO/Th 94-08 (hep-ph/9402318), to appear in Nucl. Phys. B.

[22] J. Gasser and H. Leutwyler, Ann. Phys. (N.Y.) 158 (1984) 142.

[23] H.W. Fearing and S. Scherer, preprint TRI-PP-94-68 (hep-ph/9408346).

[24] M.V. Terent'ev, Sov. J. Nucl. Phys. 16 (1973) 87.

[25] J. Kambor, talk given, reported in [36];
E. Golowich and J. Kambor, in preparation.

[26] S. Bellucci and Ch. Bruno, Frascati preprint LNF-94/037 (P).

[27] D. Babusci et al., in [34], p. 383; D. Babusci et al., Phys. Lett. B277 (1992) 158.

[28] A. Schenk, Nucl. Phys. B363 (1991) 97.

[29] J. Stern, H. Sazdjian and N.H. Fuchs, Phys. Rev. D47 (1993) 3814.

[30] P. Ko, Phys. Rev. D41 (1990) 1531; D47 (1993) 3933.

[31] J. Bijnens, S. Dawson and G. Valencia, Phys. Rev. D44 (1991) 3555.

[32] S. Bellucci and D. Babusci, in [34], p. 351.

[33] S. Bellucci, in [15], p. 419.

[34] Proceedings of the Workshop on Physics and Detectors for DAΦNE, Frascati, 1991, Ed. G. Pancheri (INFN, Frascati, 1991).

[35] M.R. Pennington, What we learn by measuring $\gamma\gamma \to \pi\pi$ at DAΦNE, this handbook; J. Portolés and M.R. Pennington, Theoretical predictions for pion polarizabilities, this handbook.

[36] R. Baldini and S. Bellucci, Pion (Kaon) and Sigma polarizabilities, in: Proceedings of the Chiral Dynamics Workshop, MIT, July 25-29, 1994, to appear;
S. Bellucci, Frascati preprint LNF-94/060 (P).

[37] B.R. Holstein, Comments Nucl. Part. Phys. 19 (1990) 221.

[38] U. Bürgi, work in progress.

[39] V.A. Petrun'kin, Sov. J. Part. Nucl. 12 (1981) 278.

[40] L.V. Fil'kov, I. Guiasu and E.E. Radescu, Phys. Rev. D26 (1982) 3146.

[41] D. Babusci et al., Phys. Lett. B314 (1993) 112.

[42] G. Höhler, in: Landolt-Börnstein, Vol. 9 b2, ed. H. Schopper, (Springer, Berlin, 1983).